

## *Full Length Research Paper*

# **A case study of the application of electrical resistivity imaging for investigation of a landslide along highway**

**Sedat YILMAZ**

Department of Geophysics, Faculty of Engineering and Architecture, Süleyman Demirel University, 32260, Isparta, Turkey. E-mail: [ssbyilmaz@yahoo.com](mailto:ssbyilmaz@yahoo.com).

Accepted 24 August, 2011

**Electrical resistivity imaging (ERI) survey was conducted in an area where landslide occurred in the Elmadag district of Ankara-Kirikkale highway and railway route, central Turkey. Landslide occurred after heavy rainfall in a rock consisting of a succession of limestone layer which was fractured. Electrical resistivity and borehole surveys were carried out to obtain the characterization and quantification of the weathered zone. The ERI sections were obtained from the dipole-dipole array. The results allowed mapping of the weathering material at depth and provided information on the depth of the sliding surface. However, the depth of the sliding surface is between 15 and 50 m.**

**Key words:** Resistivity imaging, landslide, sliding surface.

## **INTRODUCTION**

Landslides, defined as the movement of a mass of rock, debris or earth down a slope, can be triggered by a variety of external factors, such as intense rainfall, earthquake shaking, water level changes and rapid stream erosion that cause a sudden increase in shear stress or decrease in shear strength of slope-forming materials. In addition, as development expands into unstable hill-slope areas under the human activities, such as excavation of slopes for road cuts, etc., which have become important triggers for landslides. Landslides have caused the huge economic losses in highway route in central Turkey (Oztekin et al., 2006).

Although, geotechnical methods concerning the direct investigations may be used to determine landslide characteristics (Lateh et al., 2011; Mukhlisin et al., 2011), the high cost of such methods implies that they are not always suitable. A detailed structural interpretation of the landslide is not easy and sometimes impossible (Jomard et al., 2007). Combining both ERI and borehole sampling may provide better information on the subsurface structure of the landslide area (Lee et al., 2008). Borehole sampling serves as a direct observation; however, it provides only the well data. ERI method from geophysical methods is relatively cheap to give a continuous subsurface image and possible to measure

the ground response along profiles in order to obtain imaging of the subsurface. In addition, since ERI method is sensitive to the water content of layer, it is suitable to be used in landslide investigations (Bichler et al., 2004; Drahor et al., 2006; Friedel et al., 2006; Lebourg et al., 2005; Mauritsch et al., 2000; Osazuwa and Chii, 2010; Piegari et al., 2009; Roth et al., 2002; Suzuki and Higashi, 2001; Yilmaz, 2007).

Lately, improvements in commercially available equipment and computer programs allow for easier analyses that have led to new methodologies as 2D and 3D ERI (Dahlin and Zhou, 2004; Günther, 2007; Kuras et al., 2007; Loke, 2004; Loke, 2007). Multi-channel data acquisition systems have made it possible for researchers to make use of unconventional electrode array, in addition to the classical arrays, thereby enabling many simultaneous measurements to be taken for each injection point, thus significantly reducing time for data acquisition (Martorana et al., 2009). Multi-electrode ERI systems have been commonly based on data sets recorded using the electrode arrays. Each array has distinctive advantages and disadvantages in terms of sensitivity to the material variations, depth of investigation and signal strength. Sasaki (1992) determined that dipole-dipole array is more suitable for resolving complex

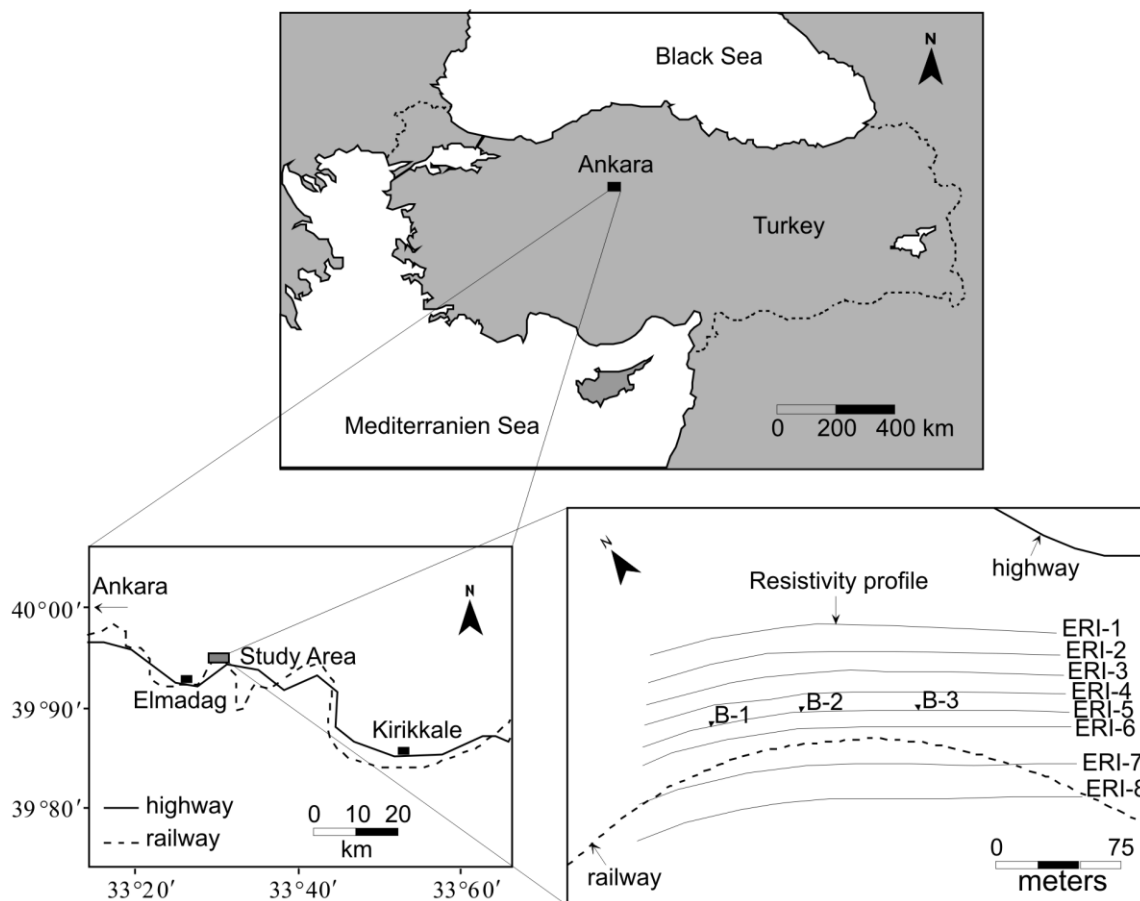


**Figure 1.** Location of study area. A zoom of this area is done in order to locate the different geophysical surveys on the more unstable part of the slope between railway and highway. Resistivity profiles indicate transversal profiles along which 2D electrical resistivity images were carried out. Borehole locations are also depicted.

structures. Oldenburg and Li (1999) stressed the differences in depth of investigation of each array in terms of the inverted models. Stummer et al. (2004) stressed that the dipole-dipole array could be used at sites where good horizontal resolution is needed.

The purpose of this work was to investigate a landslide that occurred in the Elmadag district of Ankara-Kirikkale highway and railway at 55 km in the eastward direction of Ankara, Turkey (Figure 1). This landslide is located in slope between the railway at the upper part of the landslide and the highway at the lower part of the landslide.

In the surrounding of the landslide area, the Ankara melange consists of three distinct mappable melange units, including, from Northwest to Southeast, a metamorphic melange, a limestone-block melange and an ophiolitic melange (Figure 2) (Dilek and Thy, 2006). These different melange units are imbricated along ESE-vergent thrust sheets, and the ophiolitic melange constitutes the structurally lowest tectonic unit within the Ankara melange. The metamorphic melange unit is

composed of a mixture of variably metamorphosed sedimentary and mafic-ultramafic rocks in a phyllitic-graywacke matrix. The limestone-block melange that rests tectonically on the ophiolitic melange unit is composed of Permo-Triassic neritic limestone blocks together with blocks and clasts of conglomerate, agglomerate, dolerite and flysch in a matrix composed of shale and volcanoclastic rocks. The ophiolitic melange contains kilometer-size coherent blocks of ophiolitic material that is composed of serpentized upper mantle peridotites, gabbros, doleritic dykes, pillowed to massive lava flows, radiolarian chert, and blocks and clasts of volcanic rocks, sandstone and limestone in a mainly serpentinite-made matrix (Akyürek et al., 1984; Dilek and Thy, 2006; Tankut et al., 1998).

The Ankara-Kirikkale highway is the major arterial highway between the Northeastern settlement areas and Ankara's city center. Few years ago, due to increasing traffic load and as a precaution to decrease traffic congestion in the coming years, the construction of a divided highway project was started along this highway.

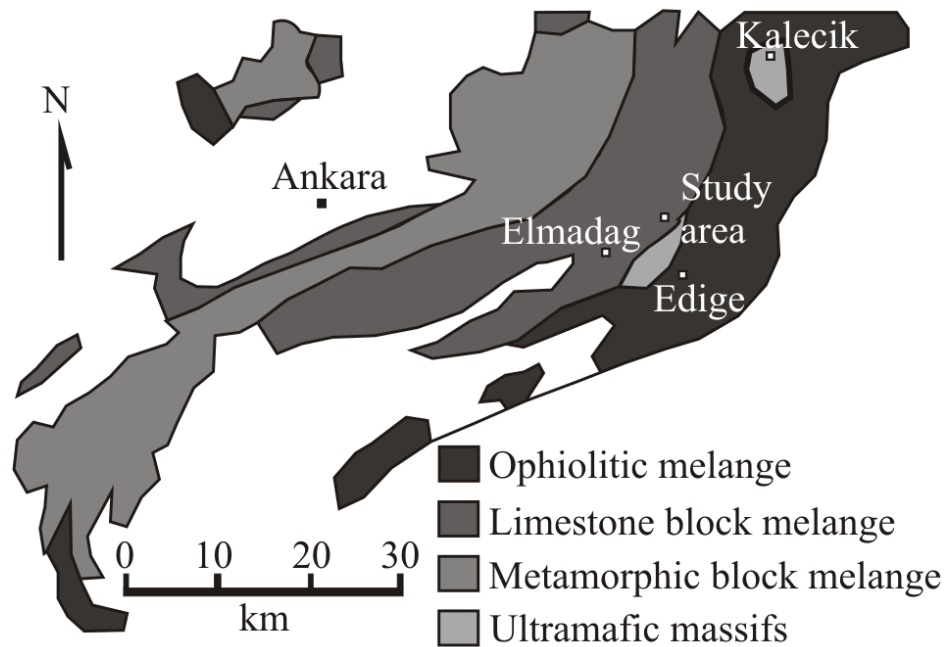


**Figure 2.** Simplified geological map of the Ankara melange in the vicinity of Elmadag town (Dilek and Thy, 2006).

Due to both widening and heavy rainfall, a landslide located near Elmadag was formed along a hill-slope between railway and highway route. Therefore, current conditions threaten local traffic safety, because of local degradation of the slope, which has a slope angle of  $15^\circ$ . Both highway and railway are threatened by the landslide and this risk has to be assessed and examined. Therefore, an ERI survey was carried out along eight lines using dipole-dipole electrode array.

### ERI DATA

The ERI method was developed to elucidate complex subsurface structures (Griffiths and Barker, 1993). It is used for obtaining a high-resolution image of subsurface patterns of electrical resistivity. To obtain a 2D image of the subsurface, it is necessary to carry out various measurements over a short period of time. This process was carried out with a multi-electrode 2D device, using 56 electrodes separated by 5 m. Dipole-dipole array with an electrode spacing of 5 m for eight resistivity profile extending 275 m was used (Figure 1).

The ERI data in the landslide area were acquired by Geophysical Service and Advanced Technologies Ltd. in January 2010. A SuperSting R8/IP automatic resistivity meter, developed by Advanced Geosciences, Inc., was used for data collection in our ERI investigation. The ERI data are traditionally presented in the form of pseudo-

section (Edwards, 1977), which give an approximate picture of the subsurface resistivity.

Inversion of the data is required to obtain a 2D true resistivity section. The ERI data were processed to generate 2D resistivity models using AGI's EarthImager 2D resistivity inversion software. EarthImager 2D discretized the subsurface model into a finite element grid. The finite element model of electrical resistivities is automatically modified through an iterative process, so that the model response converges towards the measured data (Loke and Barker, 1996). For the nonlinear inversion of the simulated data, EarthImager 2D's smooth model inversion algorithm was used, which was based on Constable et al. (1987) work. The root mean square (RMS) is a measure of its fitness between measured apparent resistivities and the apparent resistivities of the model response from the inverted resistivity (Bernstone et al., 2000).

### RESULTS AND DISCUSSION

Eight profiles, separated by a distance of approximately 15 to 20 m, were obtained on the lower zone (profiles 1 to 4) and higher part of the landslide (profiles 5 to 8) using the dipole-dipole array (Figure 1). All profiles were obtained in January 2010. The final inverted resistivity images show a RMS error of 2.99 to 10.32% after 4 to 8 iterations.

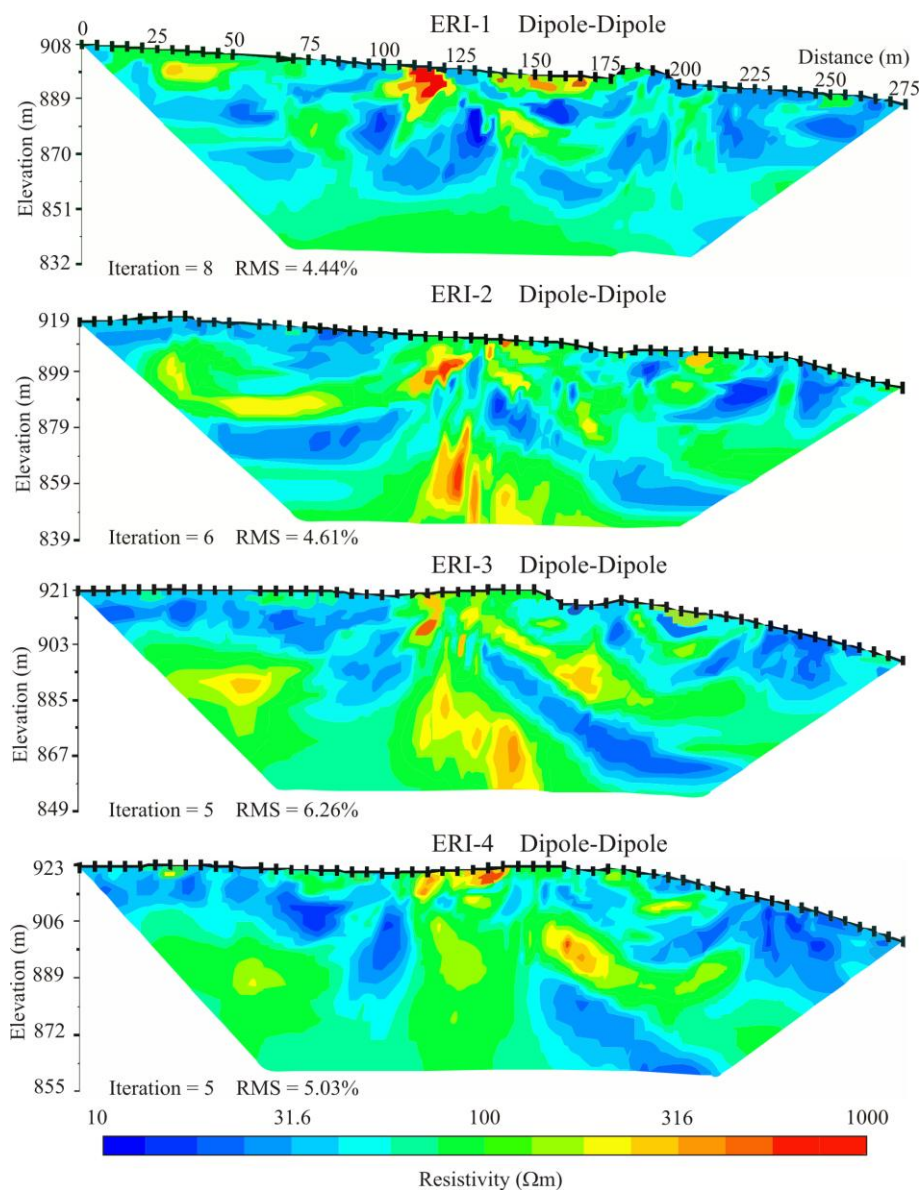


**Figure 3.** Electrical resistivity images along the profiles 1 to 4 on the lower zone of the landslide.

The eight dipole-dipole inverted resistivity images made it possible to obtain information on the variations of resistivity to a depth of 70 m. Figure 3 shows the four ERI sections obtained on the lower zone of the landslide. The ERI-1 section shows that there were relatively high resistivities (over  $200 \Omega\text{m}$ ) in places where the rock blocks were detected near the surface at the distances of 105 to 125 m and 150 to 170 m. The lower resistivity zone ( $< 30 \Omega\text{m}$ ), is the main part of the landslide mass and is between surface below and elevation 860, and is characterized by an increased moisture content and, consequently, by a weathered zone. The lower zone (about

$100 \Omega\text{m}$ ) corresponds to undisturbed unit comprising the base of the landslide. Similar results can also be recognized in the parallel survey lines ERI-2, ERI-3 and ERI-4. The high resistivity zone (over  $200 \Omega\text{m}$ ) shown in the ERI-2 and ERI-3 sections at positions 125 to 150 m corresponds to the undisturbed blocks.

Figure 4 shows the four ERI sections obtained on the higher zone of the landslide. The ERI-5 section shows that relatively high resistivities (over  $200 \Omega\text{m}$ ) corresponding rock blocks were detected near the surface at positions 65 to 180 m, in a depth of 20 to 40 m at positions 45 to 60 m, and in a depth of 25 to 65 m at

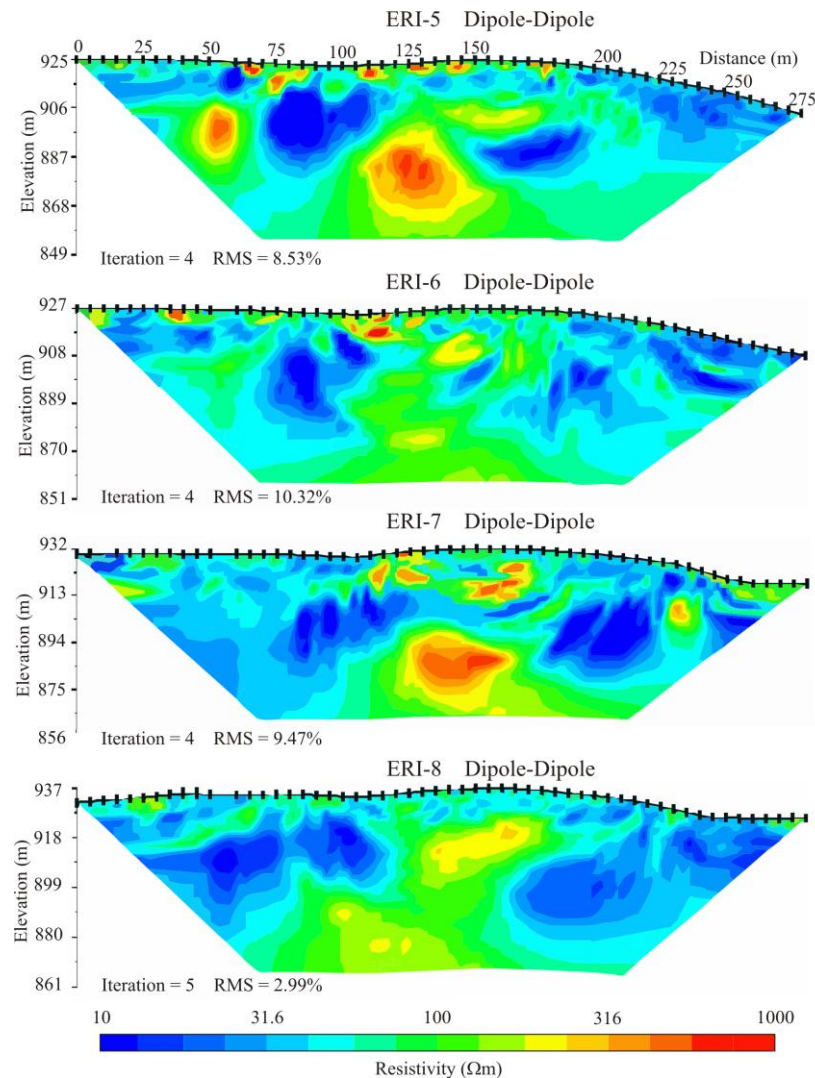


**Figure 4.** Electrical resistivity images along the profiles 5 to 8 on the higher zone of the landslide.

positions 110 to 150 m. The lower resistivity zone ( $< 30 \Omega\text{m}$ ) between the surface below and the 875 m elevation, corresponding to the landslide mass, was characterized by increased moisture content. The undisturbed unit that is characterized by moderate resistivities (around  $100 \Omega\text{m}$ ) covers all of the section. Similar results can also be recognized in the parallel survey lines ERI-6, ERI-7 and ERI-8.

Several borehole sampling related with the geotechnical investigations was performed after the landslide (Armutlu, 2010). Three boreholes located at profile 5 were drilled over the landslide materials (Figure 1). The depth range of the boreholes varies between 30 and 40 m. Each borehole is delineated on the ERI-5 dipole-dipole section according to their elevations. Figure 5 shows the interpreted dipole-dipole ERI-5 section

according to B-1, B-2 and B-3 boreholes. Comparison made between the ERI-5 section and lithology of three boreholes identified four distinct geological objects (Figure 5). Firstly, zone A of approximately 5 m thickness is characterized by moderate resistivities ( $100\text{--}300 \Omega\text{m}$ ) and is located between points 0 and 190 m. The zone is interpreted as an overburden zone consisting of gravel, sandy and silty clay. Secondly, conductive zone B of 5 to 15 m thickness is characterized by low resistivities ( $10$  to  $100 \Omega\text{m}$ ) and is located between points 0 and 190 m. The zone is interpreted as a weathered zone consisting of siltstone, claystone and limestone. Thirdly, the very low conductive zone D of approximately 20 to 30 m thickness is characterized by very low resistivities ( $10\text{m}$ ) and is located between points 70 and 125 m, and 150 m and 190 m. The very low conductive zone of approximately 50

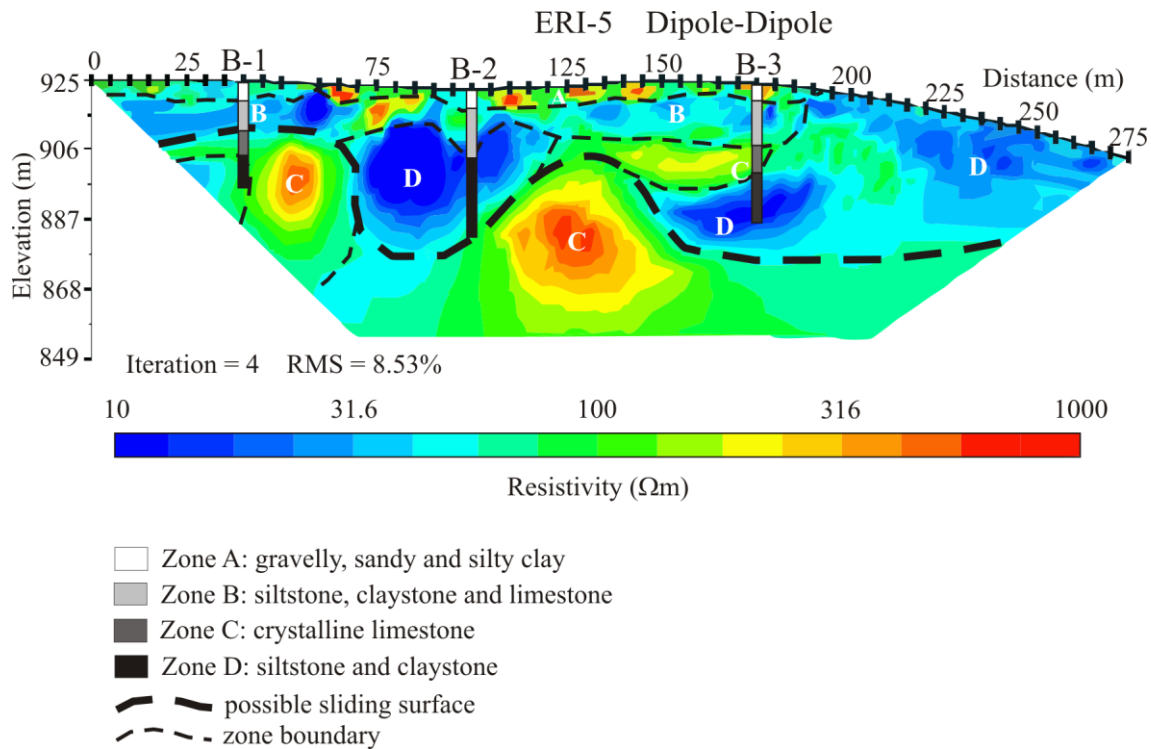


**Figure 5.** Comparison between the ERI-5 and borehole logs B-1, B-2 and B-3.

m thickness is located between points 190 and 275 m and is also represented by zone D. The zone is interpreted as the landslide mass that is characterized by increased moisture content consisting of siltstone and claystone. The limit under the zone is interpreted as sliding surface of the landslide. Lastly, the resistive zone C is characterized by high resistivities (300 to 1000  $\Omega\text{m}$ ) and is located below the horizontal points 50 and 125 m. The zone is interpreted as unweathered rock blocks consisting of crystalline limestone. The less weathered unit is characterized by resistivities around 100  $\Omega\text{m}$  surrounding these blocks that cover the entire section under the sliding surface.

## Conclusion

An electrical resistivity imaging study has been carried out over a landslide in the Elmadag district of Ankara-Kirikkale highway and railway route, central Turkey. It illustrates clearly that ERI is very helpful in studying landslides, because it provides information upon specific geoelectrical heterogeneity of the investigated zone and, thus, upon its lithological variations. An integration of the high resolution of the electrical images with borehole data permits the definition of the sliding surface and the thickness of the mobilized material. The ERI results allowed

mapping of the weathering material at depth.

A comparison between the ERI section and lithology of three boreholes has revealed sliding surface and characteristics of the landslide material. An overburden consisted of gravelly, sandy and silty clay characterized by moderate resistivities (100 to 300  $\Omega\text{m}$ ) which have about 5 m thickness. A weathered zone consisted of siltstone, claystone and limestone characterized by low resistivities (10-100  $\Omega\text{m}$ ) whose thickness is between 5 and 15 m. The very low conductive zone between 20 m and 50 m thickness characterized by very low resistivities (about 10  $\Omega\text{m}$ ) is the landslide material, and is characterized by increased moisture content consisting of siltstone and claystone. Unweathered zone consisted of crystalline limestone is characterized by high resistivities (300 to 1000  $\Omega\text{m}$ ). The less weathered unit characterized by resistivities around 100  $\Omega\text{m}$  surrounding the zone covers all of the section under the sliding surface. The transition zone between the landslide material and unweathered zone is the sliding surface at a depth varying between 15 m and 50 m. It is clear that longitudinal ERI surveying with multi-electrode arrays would be a useful in addition to this study in order to obtain subsurface structure in direction of the sliding movement. In the future, the study will be useful for a stability assessment of the landslide area. Afterwards, the ERI investigations including the other electrode arrays

will also performed for similar landslide areas.

## ACKNOWLEDGMENTS

Thanks to the Geophysical Service and Advanced Technologies Limited Company for providing data from the geophysical investigation for the Ankara-Elmadag landslide project.

## REFERENCES

- Akyurek B, Bilginer E, Akbaş B, Pehlivan Ş, Hepsen N, Sunu O, Soysal Y, Dager Z, Çatal E, Soeri B, Yildirim H, Hakyemez Y (1984). The geology of the Ankara-Elmadag-Kalecik Region. *Jeo. Muh.*, 20: 31-46.
- Armutlu G (2010). Ankara-Kırıkkale-Delice boring log. Yuksel Proje Int. Corp. Ankara (unpublished data).
- Bernstone C, Dahlin T, Ohlsson T, Hogland W (2000). DC-resistivity mapping of internal landfill structures: two pre-excavation surveys. *Env. Geol.*, 39(3-4): 360-371.
- Bichler A, Bobrowsky P, Best M, Douma M, Hunter J, Calvert T, Burns R (2004). Three-dimensional mapping of a landslide using a multi-geophysical approach: the Quesnel Forks landslide. *Landsl.* 1: 29-40.
- Constable SC, Parker RL, Constable CG (1987). Occams inversion-a practical algorithm for generating smooth models from electromagnetic sounding data. *Geophys.*, 52(3): 289-300.
- Dahlin T, Zhou B (2004). A numerical comparison of 2D resistivity imaging with 10 electrode arrays. *Geophys. Prospect.*, 52: 379-398.
- Dilek Y, Thy P (2006). Age and petrogenesis of plagiogranite intrusions in the Ankara melange, central Turkey. *Island Arc* 15: 44-57.
- Drahor MG, Gokturkler G, Berge MA, Kurtulmuş To (2006). Application of electrical resistivity tomography technique for investigation of landslides: a case from Turkey. *Env. Geol.*, 50: 147-155.
- Edwards LS (1977). A modified pseudosection for resistivity and induced-polarization. *Geophys.*, 42: 1020-1036.
- Friedel S, Thielen A, Springman SM (2006). Investigation of a slope endangered by rainfall-induced landslides using 3D resistivity tomography and geotechnical testing. *J. Appl. Geophys.*, 60(2): 100-114.
- Griffiths DH, Barker RD (1993). Two-dimensional resistivity imaging and modelling in areas of complex geology. *J. Appl. Geophys.*, 29: 211-226.
- Gunther T (2007). DC2DInvRes-Direct current 2D inversion and resolution. <http://dc2dinvres.resistivity.net>.
- Jomard H, Lebourg T, Tric E (2007). Identification of the gravitational boundary in weathered gneiss by geophysical survey: *La Clapiere* landslide (France). *J. Appl. Geophys.*, 62: 47-57.
- Kuras O, Meldum PI, Beamish D, Ogilvy RD, Lala D (2007). Capacitive resistivity imaging with towed arrays. *J. Env. Eng. Geophys.*, 12(3): 267-279.
- Lateh H, Khan MMA, Jefriza M (2011). Monitoring of shallow landslide in Tun sardon 3.9 km Pirang Island. *Int. J. Phys. Sci.*, 6(12): 2989-2999.
- Lebourg T, Binet S, Tric E, Jomard J, El Bedoui S (2005). Geophysical survey to estimate the 3D sliding surface and the 4D evolution of the water pressure on part of a Deep Seated Landslide. *Terra Nova*. 17: 399-406.
- Lee CC, Yang CH, Liu HC, Wen KL, Wang ZB, Chen YJ (2008). A study of the hydrogeological environment of the lishan landslide area using resistivity image profiling and borehole data. *Eng. Geol.*, 98: 115-125.
- Loke MH (2004). Tutorial: 2-D and 3-D electrical imaging surveys: M.H. Loke on [www.geoelectrical.com](http://www.geoelectrical.com).
- Loke MH (2007). RES2DINV ver 3.56: M.H. Loke on [www.geoelectrical.com](http://www.geoelectrical.com).
- Loke MH, Barker RD (1996). Rapid least-squares inversion of apparent resistivity pseudosections using a quasi-Newton method. *Geophys. Prospect.*, 44: 131-152.
- Martorana R, Fiandaca G, Ponsati AC, Cosentino PL (2009). Comparative tests on different multi-electrode arrays using models in near-surface geophysics. *J. Geophys. Eng.*, 6: 1-20.
- Mauritsch HJ, Seiberl W, Arndt R, Romer A, Schneiderbauer K, Sendlhofer GP (2000). Geophysical investigations of large landslides in the Carnic region of southern Austria. *Eng. Geol.*, 56: 373-388.
- Mukhlisin M, İdris I, Wan- Yaacob WZ, Elshafie A, Taha MR (2011). Soil slope deformation behavior in relation to soil water interaction based on centrifuge physical modelling. *Int. J. Phys. Sci.*, 6(13): 3126-3133.
- Oldenburg DW, Li YG (1999). Estimating depth of investigation in dc resistivity and IP surveys. *Geophys.*, 64(2): 403-416.
- Osazuwa IB, Chii EC (2010). Two-dimensional electrical resistivity survey around the periphery of an artificial lake in the Precambrian basement complex of northern Nigeria. *Int. J. Phys., Sci.* 5(3): 238-245.
- Oztekin B, Topal T, Kolat C (2006). Assessment of degradation and stability of a cut slope in limestone, Ankara-Turkey. *Eng. Geol.*, 84: 12-30.
- Piegari E, Cataudella V, Di Maio R, Milano L, Nicodemi M, Soldovieri MG (2009). Electrical resistivity tomography and statistical analysis in landslide modelling: A conceptual approach. *J. Appl. Geophys.*, 68(2): 151-158.
- Roth MJS, Mackey JR, Mackey C, Nyquist JE (2002). A case study of the reliability of multielectrode earth resistivity testing for geotechnical investigations in karst terrains. *Eng. Geol.*, 65: 225-232.
- Sasaki Y (1992). Resolution of resistivity tomography inferred from numerical simulation. *Geophys. Prospect.*, 40: 453-464.
- Stummer P, Maurer H, Gren AG (2004). Experimental design: Electrical resistivity data sets that provide optimum subsurface information. *Geophys.*, 69: 120-139.
- Suzuki K, Higashi S (2001). Groundwater flow after heavy rain in landslide-slope area from 2-D inversion of resistivity monitoring data. *Geophys.*, 49: 1708-1717.
- Tankut A, Dilek Y, Onen P (1998). Petrology and geochemistry of the Neo-Tethyan volcanism as revealed in the Ankara melange, Turkey. *J. Volc. Geoth. Res.*, 85: 265-284.
- Yilmaz S (2007). Investigation of Gürbulak landslide using 2D electrical resistivity image profiling method (Trabzon, northeastern Turkey). *J. Env. Eng. Geophys.*, 12(2): 199-205.